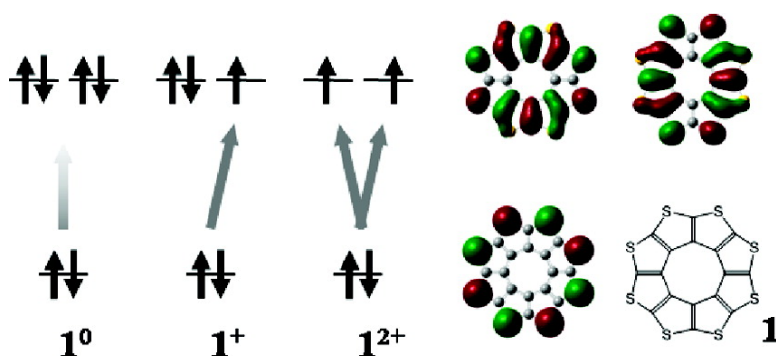


## Electrochemical and Electrochromic Properties of Octathio[8]circulene Thin Films in Ionic Liquids

Takuya Fujimoto, Michio M. Matsushita, Hirofumi Yoshikawa, and Kunio Awaga

*J. Am. Chem. Soc.*, **2008**, 130 (47), 15790-15791 • DOI: 10.1021/ja8072066 • Publication Date (Web): 01 November 2008

Downloaded from <http://pubs.acs.org> on February 8, 2009



### More About This Article

Additional resources and features associated with this article are available within the HTML version:

- Supporting Information
- Access to high resolution figures
- Links to articles and content related to this article
- Copyright permission to reproduce figures and/or text from this article

[View the Full Text HTML](#)

## Electrochemical and Electrochromic Properties of Octathio[8]circulene Thin Films in Ionic Liquids

Takuya Fujimoto, Michio M. Matsushita, Hirofumi Yoshikawa, and Kunio Awaga\*

Department of Chemistry and Research Center for Materials Science, Nagoya University, Chikusa-ku, Nagoya 464-8602, Japan

Received September 11, 2008; E-mail: awaga@mbox.chem.nagoya-u.ac.jp

Carbon–sulfur compounds<sup>1</sup> have been studied extensively as key materials in organic/molecular electronics. Octathio[8]circulene (**1**), called “sulflower,” is a new molecule (see the inset of Figure 1) that was recently synthesized by Nenajdenko et al.<sup>2</sup> This molecule is attracting much attention from various points of view: molecular symmetry caused by antiaromaticity with the  $8\pi$  electrons on the inner ring and orbital degeneracy, intermolecular packing caused by the sulfur atoms exposed to the outside of the molecular rings, and applications in organic electronics.<sup>3,4</sup> We have previously grown single crystals of this compound and carried out single-crystal X-ray analysis; the molecular structure of **1** was found to exhibit significantly suppressed antiaromaticity.<sup>5</sup> We also fabricated highly oriented thin films of **1** by vacuum evaporation.<sup>5</sup> While structural research has been carried out, the electronic structure of **1** has not yet been elucidated in detail. In this communication, we will report the electrochemistry of the thin films of **1** in ionic liquids.

Since compound **1** is insoluble in aqueous and organic solvents, it is difficult to apply conventional methods of solution electrochemistry. We therefore examined the electrochemistry of the thin films of **1** using the same method as that applied to insoluble organic polymers<sup>6,7</sup> and phthalocyanine derivatives.<sup>8–12</sup> Although the thin films of **1** easily peeled off during electrochemical reactions in organic solvents, they were stable enough to exhibit a repeatable redox process in ionic liquids such as *N,N*-diethyl-*N*-methyl(2-methoxyethyl) ammonium bis(trifluoromethylsulfonyl)imide (abbreviated as DEME-TFSI (see the inset of Figure 1)), with wide electrochemical windows.<sup>13–15</sup>

The material **1** was prepared by the method described in ref 2, and the thin films of **1** were obtained by the method in ref 5. The cyclic voltammogram (CV) was examined for the thin films (500 nm) of **1** on indium tin oxide (ITO) in DEME-TFSI, in the potential range 0.6–1.5 V vs Ag/AgCl with a slow scanning rate of 1 mV s<sup>-1</sup>. The upper limit of the potential is caused by the oxidation of DEME-TFSI. The broken curve in Figure 1 shows the results of the first run; the oxidation curve shows a gradual increase above  $E = 1.1$  V, suggesting the oxidation of **1**, but does not make a peak in the window range, probably due to the so-called overpotential effect.<sup>16</sup> It is recognized that the first redox process needs an extra potential for an irreversible penetration of counterions into films. The first reduction scan clearly exhibits two peaks at 0.95 and 0.75 V. The solid curve in Figure 1 shows the results in the second run. This curve clearly exhibits a large oxidation peak at 1.11 V and two reduction peaks at the same potentials as those in the first scan. The sum of the intensities of the two reduction peaks is nearly the same as that of the oxidation peak. In the third cycle and after, the peak positions are the same as those of the second run, but the peak intensities are slightly increased. This suggests that the redox reactions do not completely occur in the thin film and the redox

active part in it is gradually increased in this repetition. Compound **1** is concluded to be a donor, comparable to pyrene, anthracene, etc.

Figure 2a shows the UV/vis/NIR absorption spectrum for the thin film (10 nm) of **1** on quartz.<sup>17</sup> It exhibits a strong absorption at 4.7 eV in the UV range, but there is no significant absorption peak in the visible range, namely below 3 eV. During the CV measurements, the thin films of **1** undergo a significant color change, as indicated in the inset of Figure 2. The thin film at 0.0 V looks faint red, but this color is probably caused by an interference effect due to the film thickness of 500 nm. After the oxidation, the color

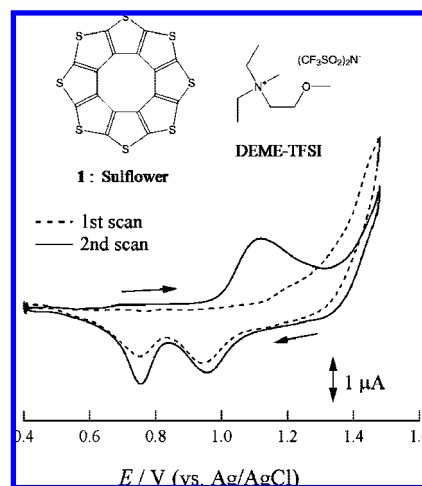


**Figure 1.** Cyclic voltammogram of a thin film of **1** on ITO with a scanning rate of 1 mV s<sup>-1</sup>. The inset shows the molecular structures of **1** and DEME-TFSI.

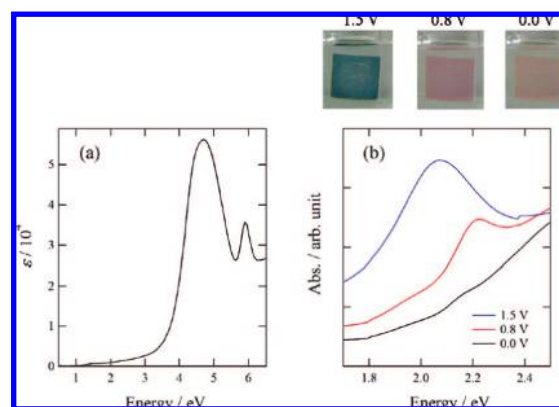


**Figure 2.** (a) UV/vis/NIR absorption spectrum for the thin film of **1** (10 nm) on quartz. (b) *In situ* absorption spectra for the thin film of **1** (500 nm) on ITO in DEME-TFSI in the reduction scan at  $E = 1.5, 0.8,$  and  $0.0$  V. The inset shows the photographs at these potentials.

turns to blue at 1.5 V. In the reduction process from this potential, the color becomes dark red at 0.8 V and then colorless (faint red) at 0.0 V.

We carried out *in situ* UV/vis/NIR absorption measurements in the photon energy 1.4–4.0 eV for the thin film (500 nm) of **1** in the reduction scan at  $E = 1.5$ , 0.8 and 0.0 V. Due to the strong absorptions of ITO and DEME-TFSI, we could not obtain reliable data above 4.0 eV and below 1.4 eV. The results for the ranges 1.4–4.0 and 1.7–2.5 eV are shown in Figures S1 and 2b, respectively, while the absorptions of ITO and DEME-TFSI are not compensated in them. The black curve at  $E = 0.0$  V corresponds to the absorption of the neutral species  $\mathbf{1}^0$ ; there is no absorption peak in this range. The blue curve at  $E = 1.6$  V and the red curve at 0.8 V exhibit absorption peaks at 2.07 and 2.21 eV, respectively, while the intensity of the former is much larger than that of the latter.

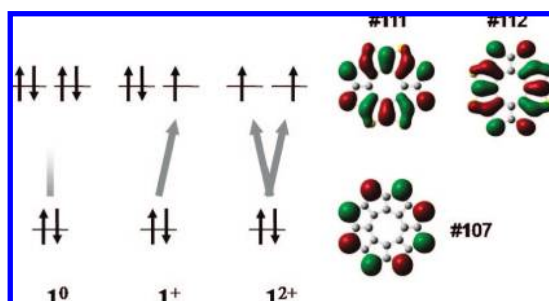


**Figure 3.** The molecular orbitals corresponding to the absorption bands in Figure 2. The molecular orbitals, #111 and #112, are the nearly degenerated HOMOs of the neutral molecule  $\mathbf{1}^0$ , while #107 is a nonbonding orbital localized on the sulfur atoms.

To interpret the electrochromism of **1**, we carried out the molecular orbital calculations (TD-DFT B3LYP method with a 6-31G(d) basis set) for  $\mathbf{1}^0$ ,  $\mathbf{1}^+$ , and  $\mathbf{1}^{2+}$ . Figure S2 shows the theoretically expected absorption spectra for the three species. The figure shows that the neutral molecule  $\mathbf{1}^0$  exhibits no absorption in the range 1.7–4.0 eV, which agrees well with the experimental results (Figure 2a). In contrast, the monocation species  $\mathbf{1}^+$  is suggested to exhibit a weak absorption at 2.24 eV ( $f = 0.121$ ) in this energy range. The dication species  $\mathbf{1}^{2+}$  is theoretically predicted to possess a triplet ground state and to exhibit two nearly superimposed weak absorptions at 2.11 eV ( $f = 0.139$  and 0.140). These weak absorptions of  $\mathbf{1}^+$  and  $\mathbf{1}^{2+}$  have the same origin; they are mainly caused by the transition from the molecular orbital #107 to the nearly degenerated orbitals #111 and #112, as shown in Figure 3. Orbital #107 is a nonbonding orbital, localized on the sulfur atoms, while #111 and #112 are the nearly degenerated HOMOs of the neutral species  $\mathbf{1}^0$ . The transition from #107 to #111 or #112 is forbidden in  $\mathbf{1}^0$  because there is no vacancy in #111 and #112. In contrast, since there are one and two vacancies in #111 and #112 for  $\mathbf{1}^+$  and  $\mathbf{1}^{2+}$ , respectively, this transition is allowed in them and the absorption in  $\mathbf{1}^{2+}$  is twice as strong as that in  $\mathbf{1}^+$  (see Figure 3). The theoretically expected optical absorptions of  $\mathbf{1}^+$  and  $\mathbf{1}^{2+}$  can well reproduce the absorptions at  $E = 0.8$  V (red curve) and 1.5 V (blue curve) in Figure 2b, respectively, with regard to both peak position and relative intensity. It is concluded that the CV curves in Figure 1 include two-electron oxidation at  $E = 1.11$  V ( $\mathbf{1}^0 \rightarrow \mathbf{1}^{2+}$ ) and stepwise reductions at  $E = 0.95$  ( $\mathbf{1}^{2+} \rightarrow \mathbf{1}^+$ ) and 0.75 V ( $\mathbf{1}^+ \rightarrow \mathbf{1}^0$ ). Such a one-step two-electron oxidation/reduction is occasionally found in some specific molecules with degenerated

HOMOs/LUMOs.<sup>18,19</sup> It is hard to clearly rationalize the stepwise reductions of  $\mathbf{1}^{2+}$ , but one possible reason is different geometries of the two counteranions around  $\mathbf{1}^{2+}$  in the thin film.

We carried out *in situ* resistivity  $R$  measurements for the thin films of **1**, using the interdigitated array electrodes (Pt) with a gap width of 2  $\mu\text{m}$  and an alternating current. Since the thin films were not very stable on the interdigitated electrodes and easily peeled off during the measurements, we could not carry out the measurements in the second redox cycle and after. Figure S3 depicts the potential dependence of the resistivity in the first oxidation; the values of  $R$  show a decrease by 2 orders of magnitude and a minimum at  $E = 1.3$  V. These *in situ* resistivity measurements suggest that the material **1** is a potential conductor, applicable to solid-state organic/molecular electronics.

In summary, we studied the electrochemistry of the thin films of **1** in an ionic liquid DEME-TFSI. This method, applicable to various insoluble materials with strong self-assembling forces, easily revealed the redox process of **1** with significant electrochromism. This color change, well-interpreted in terms of the allowed  $n-\pi$  transition by electrochemical oxidation, was good experimental evidence for the nearly degenerated HOMOs in **1**. We believe that compound **1** with orbital degeneracy and 3D crystal structure<sup>5</sup> has a high potential to yield unusual electronic and/or magnetic properties.

**Acknowledgment.** This work was supported by a Grant-in-Aid for Scientific Research from the Ministry of Education, Culture, Sports, Science, and Technology (MEXT).

**Supporting Information Available:** Spectroscopic and *in situ* resistance data. This material is available free of charge via the Internet at <http://pubs.acs.org>.

## References

- (1) Torroba, T.; Garcia-Valverde, M. *Angew. Chem., Int. Ed.* **2006**, *45*, 8092–8096, and references therein.
- (2) Chernichenko, K. Y.; Sumerin, V. V.; Shpanchenko, R. V.; Balenkova, E. S.; Nenajdenko, V. G. *Angew. Chem., Int. Ed.* **2006**, *45*, 7367–7370.
- (3) Datta, A.; Pati, S. K. *J. Phys. Chem. C* **2007**, *111*, 4487–4490.
- (4) Gahungu, G.; Zhang, J. *Phys. Chem. Chem. Phys.* **2008**, *10*, 1743–1747.
- (5) Fujimoto, T.; Suizu, R.; Yoshikawa, H.; Awaga, K. *Chem.–Eur. J.* **2008**, *14*, 6053–6056.
- (6) Marks, T. J.; Gaudiello, J. G.; Kellogg, G. E.; Tetrick, S. M. *ACS Symp. Ser.* **1988**, *360*, 224–237.
- (7) Mortimer, R. J. *Chem. Soc. Rev.* **1997**, *26*, 147–156.
- (8) (a) Toshima, N.; Kawamura, S.; Tominaga, T. *Chem. Lett.* **1993**, 1299–1302. (b) Toshima, N.; Tominaga, T.; Kawamura, S. *Bull. Chem. Soc. Jpn.* **1996**, *69*, 245–253. (c) Toshima, N.; Tominaga, T. *Bull. Chem. Soc. Jpn.* **1996**, *69*, 2111–2122.
- (9) (a) Kahl, J. L.; Faulkner, L. R.; Dwarakanath, K.; Tachikawa, H. *J. Am. Chem. Soc.* **1986**, *108*, 5434–5440. (b) Green, J. M.; Faulkner, L. R. *J. Am. Chem. Soc.* **1983**, *105*, 2950–2955.
- (10) Brown, K. L.; Mottola, H. A. *Langmuir* **1998**, *14*, 3411–3417.
- (11) (a) Silver, J.; Lukes, P.; Houlton, A.; Howe, S.; Hey, P.; Ahmet, M. T.; Mustafa, T. *J. Mater. Chem.* **1992**, *2*, 849–855. (b) Silver, J.; Lukes, P.; Hey, P.; Ahmet, M. T. *J. Mater. Chem.* **1992**, *2*, 841–847.
- (12) Miyoshi, Y.; Kubo, M.; Fujinawa, T.; Suzuki, Y.; Yoshikawa, H.; Awaga, K. *Angew. Chem., Int. Ed.* **2007**, *46*, 5532–5536.
- (13) Wilkes, J. S.; Zaworotlo, M. J. *Chem. Commun.* **1992**, 965.
- (14) Sato, T.; Masuda, G.; Takagi, K. *Electrochim. Acta* **2004**, *49*, 3603–3611.
- (15) Seki, S.; Ohno, Y.; Miyashiro, H.; Kobayashi, Y.; Usami, A.; Mita, Y.; Terada, N.; Hayamizu, K.; Tsuzuki, S.; Watanabe, M. *J. Electrochem. Soc.* **2008**, *155*, A421–A427, and references therein.
- (16) (a) Kalaji, M.; Peter, L. M.; Abrantes, L. M.; Mesquita, J. S. *J. Electroanal. Chem.* **1989**, *274*, 289–295. (b) Odin, C.; Nechtschein, M. *Synth. Met.* **1991**, *41–43*, 2943–2946. (c) Barbero, C.; Kötz, R.; Kalaji, M.; Nyholm, L.; Peter, L. M. *Synth. Met.* **1993**, *55–57*, 1545–1551.
- (17) The  $\epsilon$  values were calculated, using the molecular weight (448.70) and the density (2.096 g/cm<sup>3</sup>) of **1**.
- (18) Takahashi, K. *Pure Appl. Chem.* **1993**, *65*, 127–134.
- (19) Kvarnström, C.; Neugebauer, H.; Kuzmany, H.; Sitter, H.; Sariciftci, N. S. *J. Electroanal. Chem.* **2001**, *511*, 13–19.

JA8072066